Synthesis, Structural Characterization, and Photophysics of Dinuclear Gold(II) Complexes $[\{Au(dppn)Br\}_2](PF_6)_2$ and $[\{Au(dppn)I\}_2](PF_6)_2$ with an Unsupported $Au^{II}-Au^{II}$ Bond

Vivian Wing-Wah Yam,* Chi-Kwan Li, Chui-Ling Chan, and Kung-Kai Cheung

Department of Chemistry, The University of Hong Kong, Pokfulam Road, Hong Kong, P. R. China

Received July 12, 2001

A series of novel dinuclear gold(II) complexes having an unsupported Au(II)−Au(II) bond with well-defined oxidation state at the gold center were synthesized. Red shifts in both the low-energy absorption and emission bands were observed upon increasing the donor ability of the coordinated halogen atoms.

Introduction

The +2 oxidation state of gold with electronic configuration $[Xe]4f^{14}5d^9$ is less common for gold than for copper. Many complexes which, from empirical formula, appear to be Au(II) complexes are actually mixed oxidation states of Au(I)−Au(III) complexes; for example, $CsAuCl_3$ should be $Cs_2[AuCl_2][AuCl_4]$.[1] The most well-known dinuclear gold(II) complexes containing formal single bond are gold(II) ylide complexes[2] and gold(II) complexes with the unsaturated sulfur donor ligands *N*,*N*-dialkyldithiocarbamate (dtc^-)[3] and maleonitriledithiolate (mnt^{2-}).[4] The general synthesis of these complexes involved the oxidative addition of halogen to the corresponding dinuclear gold(I) derivatives.[4a,5] However, examples of complexes possessing a direct formal Au−Au bond unbridged by any other ligand are rare in the literature.[2,6] Recently, we reported the synthesis and structural characterization of a novel dinuclear gold(II) complex $[\{Au^{II}(dppn)Cl\}_2](PF_6)_2$, which represents the first example of a cationic complex having an unsupported Au(II)−Au(II) bond.[7] Solid and solution samples of this complex as well as most of the other gold(II) complexes show a very distinctive deep red to blue color,[2i,4a] which is not commonly observed in the gold(I) or gold(III) analogues. To provide insights into the nature of these transitions, we have extended our work to the preparation of the structurally related halo analogues. Herein are reported the synthesis and structural characterization of the two halo analogues, $[\{Au^{II}(dppn)X\}_2](PF_6)_2$ (X = Br (**1**), I (**2**)) (Chart 1), and their spectroscopic studies. A comparison of the structural and spectroscopic properties of these complexes with their chloro counterpart, $[\{Au^{II}(dppn)Cl\}_2](PF_6)_2$, has been made to provide insights into their spectroscopic origin.

Chart 1. Structure of $[\{Au^{II}(dppn)X\}_2](PF_6)_2$, where X = Cl, Br (**1**), and I (**2**)

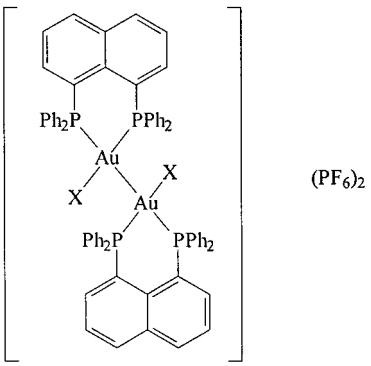

Experimental Section

Materials. Tetrakis(acetonitrile)silver(I) hexafluorophosphate[8] and 1,8-bis(diphenylphosphino)naphthalene (dppn)[9] were prepared according to reported methods. $HAuBr_4$[10] and $(^nBu_4N)[AuI_2]$[11] were synthesized according to literature procedures. $[Au_2(dppn)Br_2]$ and $[Au_2(dppn)I_2]$ were prepared according to a modification of the literature procedures by reacting $HAuBr_4$ with dppn in the presence of 2,2′-thiodiethanol[12] in methanol and by reacting $(^nBu_4N)[AuI_2]$ with dppn in ethanol,[13] respectively. All other solvents and reagents were of analytical grade and were used as received.

(1) Elliot, N.; Pauling, L. *J. Am. Chem. Soc.* **1938**, *60*, 1846.
(2) (a) Murray, H. H.; Fackler, J. P., Jr.; Porter, L. C.; Briggs, D. A.; Guerra, M. A.; Lagow, R. J. *Inorg. Chem.* **1987**, *26*, 357. (b) Schmidbaur, H.; Mandl, J. R.; Frank, A.; Huttner, G. *Chem. Ber.* **1976**, *109*, 466. (c) Usón, R.; Laguna, A.; Laguna, M.; Jimenez, J.; Jones, P. G. *Angew. Chem., Int. Ed. Engl.* **1991**, *30*, 198. (d) Usón, R.; Laguna, A.; Laguna, M.; Jimenez, J.; Jones, P. G. *J. Chem. Soc., Dalton Trans.* **1991**, 1361. (e) Bardaji, M.; Connelly, N. G.; Gimeno, M. C.; Jones, P. G.; Laguna, A.; Laguna, M. *J. Chem. Soc., Dalton Trans.* **1995**, 2245. (f) Murray, H. H.; Mazany, A. M.; Fackler, J. P., Jr. *Organometallics* **1985**, *4*, 154. (g) Usón, R.; Laguna, A.; Laguna, M.; Fraile, M. N. *J. Chem. Soc., Dalton Trans.* **1986**, 291. (h) Usón, R.; Laguna, A.; Laguna, M.; Tartón, M. T.; Jones, P. G. *J. Chem. Soc., Chem. Commun.* **1988**, 740. (i) Basil, J. D.; Murray, H. H.; Fackler, J. P., Jr.; Tocher, J.; Mazany, A. M.; Bancroft, B. T.; Knachel, H.; Dudis, D.; Delord, T. J.; Marler, D. O. *J. Am. Chem. Soc.* **1985**, *107*, 6908. (j) King, C.; Heinrich, D. D.; Garzon, G.; Wang, J. C.; Fackler, J. P., Jr. *J. Am. Chem. Soc.* **1989**, *111*, 2300.
(3) Calabro, D. C.; Harrison, B. A.; Palmer, G. T.; Moguel, M. K.; Rebbert, R. L.; Burmeister, J. L. *Inorg. Chem.* **1981**, *20*, 4311.
(4) (a) Khan, M. N.; Wang, S.; Fackler, J. P., Jr. *Inorg. Chem.* **1989**, *28*, 3579. (b) Khan, M. N.; Fackler, J. P., Jr.; King, C.; Wang, J. C.; Wang, S. *Inorg. Chem.* **1988**, *27*, 1672.
(5) Schmidbaur, H.; Franke, R. *Inorg. Chim. Acta* **1975**, *13*, 85.
(6) Gimeno, M. C.; Jimenez, J.; Jones, P. G.; Laguna, A.; Laguna, M. *Organometallics* **1994**, *13*, 2508.
(7) Yam, V. W. W.; Choi, S. W. K.; Cheung, K. K. *J. Chem. Soc., Chem. Commun.* **1996**, 1173.
(8) Åkermark, B.; Vitagliano, A. *Organometallics* **1985**, *4*, 1281.
(9) Jackson, R. D.; James, S.; Orpen, A. G.; Pringle, P. G. *J. Organomet. Chem.* **1993**, *458*, C3.
(10) Block, B. P.; Bartkiewicz, S. A.; Chrisp, J. D. *Inorg. Synth.* **1953**, *4*, 14.
(11) Braunstein, P.; Clark, R. J. H. *J. Chem. Soc., Dalton Trans.* **1973**, 1845.
(12) (a) Yam, V. W. W.; Choi, S. W. K. *J. Chem. Soc., Dalton Trans.* **1994**, 2057. (b) Schmidbaur, H.; Wagner, F. E.; Hammer, A. W. *Chem. Ber.* **1979**, *112*, 496.
(13) Angermair, K.; Bowmaker, G. A.; Silva, E. N.; Healy, P. C.; Jones, B. E.; Schmidbaur, H. *J. Chem. Soc., Dalton Trans.* **1996**, 3121.

10.1021/ic010744t CCC: $20.00
Published on Web 11/16/2001

All reactions were carried out in an atmosphere of nitrogen using standard Schlenk techniques.

Physical Measurements and Instrumentation. ^{1}H and ^{31}P{^{1}H} NMR spectra were recorded on Bruker DPX-300 (300 MHz) and DRX-500 (202 MHz) FT-NMR spectrometers, respectively. Chemical shifts for ^{1}H NMR were reported relative to tetramethylsilane while that of ^{31}P{^{1}H} NMR were reported relative to 85% H_3PO_4. Electrospray-ionization mass spectra were recorded on a Finnigan LCQ mass spectrometer. The infrared spectra were obtained as Nujol mull on KBr disk on a Bio-Rad FTS-7 IR spectrophotometer. Elemental analyses of all the complexes were performed on a Carlo Erba 1106 elemental analyzer at the Institute of Chemistry at the Chinese Academy of Sciences in Beijing. Electronic absorption spectra were recorded on a Hewlett-Packard 8452A diode array spectrophotometer. Steady-state emission and excitation spectra recorded at room temperature were obtained on a Spex Fluorolog-2 model F 111 fluorescence spectrophotometer with or without Corning filters.

Synthesis. [{Au^{II}(dppn)Br}$_2$](PF$_6$)$_2$ (1). Similar to the preparation of [{Au^{II}(dppn)Cl}$_2$](PF$_6$)$_2$,[7] [Ag(MeCN)$_4$]PF$_6$ (113 mg, 0.27 mmol) and dppn (94 mg, 0.19 mmol) were added to a suspension of [Au$_2$(dppn)Br$_2$] (100 mg, 0.10 mmol) in acetonitrile (5 mL) at room temperature. The dull orange suspension changed rapidly into a turbid deep purple solution, and the mixture was stirred for 15 min. The gray suspension was then filtered, and the solvent was removed under reduced pressure. The purple residue was then recrystallized from dichloromethane−diethyl ether to give air-stable dark purple crystals (50 mg, 0.03 mmol, 29% yield). ^{1}H NMR (300 MHz, CD_2Cl_2, 298 K): δ 6.20 (d, 2H, J = 7.50 Hz, Np), 6.26 (d, 2H, J = 7.37 Hz, Np), 6.85−6.95 (m, 4H, Np), 7.20−8.10 (m, 40H, PPh$_2$), 8.63 (d, 2H, J = 7.85 Hz, Np), 8.73 (d, 2H, J = 7.95 Hz, Np). ^{31}P{^{1}H} NMR (202 MHz, CD_2Cl_2, 298 K): δ 29.5 (s), 7.2 (s). ^{31}P{^{1}H} NMR (202 MHz, CD_2Cl_2, 203 K): δ 28.8 (s), 6.8 (s). Positive ESI-MS: m/z 1690 [(M − PF$_6$)$^+$]. IR (Nujol): ν/cm^{-1} 842 s (ν_{P-F}). Anal. Found: C, 42.91; H, 2.77. Calcd for $C_{68}H_{52}P_6Au_2Br_2F_{12}\cdot CH_2Cl_2$: C, 43.13; H, 2.83.

[{Au^{II}(dppn)I}$_2$](PF$_6$)$_2$ (2). Similar to the preparation of [{Au^{II}(dppn)Cl}$_2$](PF$_6$)$_2$,[7] [Ag(MeCN)$_4$]PF$_6$ (218 mg, 0.52 mmol), dppn (86.8 mg, 0.17 mmol) and iodine (44.4 mg, 0.17 mmol) were added to a suspension of [Au$_2$(dppn)I$_2$] (100 mg, 0.09 mmol) (prepared from (^{n}Bu$_4$N)[AuI$_2$] and dppn in ethanol) in acetonitrile (5 mL) at room temperature. The dull green suspension changed rapidly to a turbid deep blue-purple solution. After being stirred for 15 min, the suspension was filtered and the solvent was removed under reduced pressure. The dark purple residue was then recrystallized from acetonitrile−diethyl ether to give air-stable dark purple crystals (43 mg, 0.02 mmol, 25% yield). ^{1}H NMR (300 MHz, CD_2Cl_2, 298 K): δ 6.20−6.45 (m, 4H, Np), 6.80−7.00 (m, 4H, Np), 7.30−8.10 (m, 40H, PPh$_2$), 8.62 (d, 2H, J = 6.80 Hz, Np), 8.72 (d, 2H, J = 6.47 Hz, Np). ^{31}P{^{1}H} NMR (202 MHz, CD_2Cl_2, 298 K): δ 24.9 (s), −6.8 (br s). ^{31}P{^{1}H} NMR (202 MHz, CD_2Cl_2, 203 K): δ 25.0 (s), −5.8 (s). Positive ESI-MS: m/z 1784 [(M − PF$_6$)$^+$]. IR (Nujol): ν/cm^{-1} 840 s (ν_{P-F}). Anal. Found: C, 43.26; H, 2.90. Calcd for $C_{68}H_{52}P_6Au_2I_2F_{12}\cdot(CH_3CH_2)_2O$: C, 43.13; H, 3.12.

Crystal Structure Determination. Single crystals of both complexes **1** and **2** were obtained by diffusion of diethyl ether vapor into an acetonitrile solution of the complex.

Crystal data for 1: [$(C_{68}H_{52}P_4Br_2Au_2)^{2+}(PF_6^-)_2\cdot 3CH_3CN$], formula weight = 1959.88, triclinic, space group $P\bar{1}$ (No. 2), a = 13.914(2) Å, b = 15.369(3) Å, c = 19.572(3) Å, α = 103.49(2)°, β = 103.11(2)°, γ = 95.54(2)°, V = 3914(1) Å^3, Z = 2, D_c = 1.663 g cm^{-3}, μ(Mo Kα) = 49.74 cm^{-1}, F(000) = 1904, T = 301 K. An orange crystal of dimensions 0.25 × 0.15 × 0.10 mm mounted in a glass capillary was used for data collection at 28 °C on a MAR diffractometer with a 300 mm image plate detector using graphite-monochromatized Mo Kα radiation (λ = 0.710 73 Å). Data collection was made with 2° oscillation (105 images) at 120 mm distance and 600 s exposure. The images were interpreted and intensities integrated using program DENZO.[14] A total of 12 077 unique reflections were obtained from a total of 41 372 measured reflections (R_{int} = 0.068). A total of 7183 reflections with $I > 3\sigma(I)$ were considered observed and used in the structural analysis. These reflections were in the following range: h, 0 to 15; k, −18 to 18; l, −23 to 22 ($2\theta_{max}$ = 52.4°). The space group was uniquely determined based on statistical analysis of intensity distribution and successful refinement of structure solved by Patterson methods and expanded by Fourier methods (PATTY[15]) and refinement by full-matrix least-squares using the software package TeXsan[16] on a Silicon Graphics Indy computer. A crystallographic asymmetric unit consists of one formula unit. In the least-squares refinement, 78 non-H atoms were refined anisotropically, the 12 F atoms and non-H atoms of the solvent molecules were refined isotropically, and 61 H atoms at calculated positions with thermal parameters equal to 1.3 times that of the attached C atoms were not refined. Convergence for 787 variable parameters by least-squares refinement on F with $w = 4F_o^2/\sigma^2(F_o^2)$, where $\sigma^2(F_o^2) = [\sigma^2(I) + (0.040F_o^2)^2]$ for 7183 reflections with $I > 3\sigma(I)$ was reached at R = 0.058 and R_w = 0.078 with a goodness-of-fit of 1.70. $(\Delta/\sigma)_{max}$ = 0.05 except for atoms of the solvent molecules. The final difference Fourier map was featureless, with maximum positive and negative peaks of 1.24 and 1.77 e Å^{-3}, respectively.

Crystal data for 2: [$(C_{68}H_{52}P_4I_2Au_2)^{2+}(PF_6^-)_2\cdot C_2H_5OH$], formula weight = 1976.79, triclinic, space group $P\bar{1}$ (No. 2), a = 13.942(2) Å, b = 17.062(3) Å, c = 18.648(3) Å, α = 65.77(2)°, β = 74.48(2)°, γ = 67.64(2)°, V = 3708(1) Å^3, Z = 2, D_c = 1.770 g cm^{-3}, μ(Mo Kα) = 49.98 cm^{-1}, F(000) = 1896, T = 301 K. A dark brown crystal of dimensions 0.45 × 0.07 × 0.05 mm mounted in a glass capillary was used for data collection at 28 °C on a MAR diffractometer with a 300 mm image plate detector using graphite-monochromatized Mo Kα radiation (λ = 0.710 73 Å). Data collection was made with 2° oscillation (105 images) at 120 mm distance and 600 s exposure. The images were interpreted and intensities integrated using program DENZO.[14] A total of 12 130 unique reflections were obtained from a total of 42 686 measured reflections (R_{int} = 0.059). A total of 7713 reflections with $I > 3\sigma(I)$ were considered observed and used in the structural analysis. These reflections were in the following range: h, 0 to 15; k, −18 to 20; l, −21 to 22 ($2\theta_{max}$ = 51.0°). The space group was determined on the basis of statistical analysis of intensity distribution and the successful refinement of structure solved by Patterson methods and expanded by Fourier methods (PATTY[15]) and refinement by full-matrix least-squares using the software package TeXsan[16] on a Silicon Graphics Indy computer. A crystallographic asymmetric unit consists of one formula unit. One F atom of each PF_6 anion was distorted and was placed at two positions with F(6), F(6′), F(12), and F(12′) having occupation numbers of 0.5, 0.5, 0.6, and 0.4, respectively. In the least-squares refinement, 78 non-H atoms were refined anisotropically, the 14 F atoms and non-H atoms of the ethanol molecules were refined isotropically, and 57 H atoms at calculated positions with thermal parameters equal to 1.3 times that of the attached C atoms were not refined. The hydroxy H atom of the ethanol molecule was not included in the calculation. Convergence for 771 variable parameters by least-squares refinement on F with $w = 4F_o^2/\sigma^2(F_o^2)$, where $\sigma^2(F_o^2) = [\sigma^2(I) + (0.033F_o^2)^2]$ for 7713 reflections with $I > 3\sigma(I)$ was reached at R = 0.056 and R_w = 0.074 with a goodness-of-fit of 1.88. $(\Delta/\sigma)_{max}$ = 0.05 except for atoms of the solvent molecule. The final difference Fourier map was featureless, with maximum positive and negative peaks of 1.34 and 1.73 e Å^{-3}, respectively.

The crystal data and details of collection and refinement for the complexes **1** and **2** are summarized in Table 1.

Results and Discussion

Syntheses and Characterization. Complexes **1** and **2** were synthesized by modification of an earlier procedure on the chloro

(14) Gewirth, D. DENZO. In *The HKL Manual-A description of programs DENZO, XDISPLAYF, and SCALEPACK*; written by with the cooperation of the program authors Z. Otwinowski and W. Minor; Yale University: New Haven, CT, 1995.

(15) Beurskens, P. T.; Admiraal, G.; Beurskens, G.; Bosman, W. P.; Garcia-Granda, S.; Gould, R. O.; Smits, J. M. M.; Smykalla, C. *PATTY, The DIRDIF program system*; Technical Report of the Crystallography Laboratory, University of Nijmegen, Nijmegen, The Netherlands, 1992.

(16) *TeXsan*: *Crystal Structure Analysis Package*; Molecular Structure Corp.: The Woodlands, TX, 1985, 1992.

Table 1. Crystallographic Data for $[\{Au^{II}(dppn)Br\}_2](PF_6)_2$ (**1**) and $[\{Au^{II}(dppn)I\}_2](PF_6)_2$ (**2**)

	1	**2**
formula	$[(C_{68}H_{52}P_4Br_2Au_2)^{2+}(PF_6)_2\cdot 3CH_3CN]$	$[(C_{68}H_{52}P_4I_2Au_2)^{2+}(PF_6)_2\cdot C_2H_5OH]$
fw	1959.88	1976.79
cryst system	triclinic	triclinic
space group	$P\bar{1}$ (No. 2)	$P\bar{1}$ (No. 2)
color	orange	dark brown
cryst size, mm	0.25 × 0.15 × 0.10	0.45 × 0.07 × 0.05
a, Å	13.914(2)	13.942(2)
b, Å	15.369(3)	17.062(3)
c, Å	19.572(3)	18.648(3)
α, deg	103.49(2)	65.77(2)
β, deg	103.11(2)	74.48(2)
γ, deg	95.54(2)	67.64(2)
V, Å^3	3914(1)	3708(1)
Z	2	2
T, K	301	301
D_c (g cm^{-3})	1.663	1.770
μ, cm^{-1}	49.74	49.98
F(000)	1904	1896
$2\theta_{max}$, deg	52.4	51.0
R, R_w[a]	0.058, 0.078	0.056, 0.074

[a] $w = 4F_o^2/[\sigma^2(I) + (aF_o^2)^2]$ with $I > 3\sigma(I)$ (**1**, $a = 0.040$; **2**, $a = 0.033$).

analogue, $[\{Au(dppn)Cl\}_2](PF_6)_2$, reported by us.[7] Reaction of $[Au_2(dppn)Br_2]$ with an excess of $[Ag(MeCN)_4]PF_6$ and dppn in acetonitrile gave a deep purple solution of **1**, which was then filtered, evaporated to dryness, and recrystallized from dichloromethane−diethyl ether to give deep purple crystals of **1**. A side product of $[Au(dppn)_2]PF_6$ was obtained from the filtrate after the isolation of **1**. $[Ag(MeCN)_4]PF_6$ serves as the oxidizing agent to oxidize the Au^I centers to Au^{II} and itself being reduced to metallic Ag^0. In the case of **2**, an additional amount of iodine was added to serve as both the oxidizing agent and as a source of iodide ions to enhance the formation and stability of the gold(II)−iodide complex. Both complexes gave satisfactory elemental analyses and have been characterized by ^{1}H NMR, $^{31}P\{^1H\}$ NMR, IR, and positive ESI-MS. The $^{31}P\{^1H\}$ NMR spectra of **1**, **2**, and their chloro analogue, $[\{Au(dppn)Cl\}_2](PF_6)_2$,[17] all show two singlets at 298 and 203 K, corresponding to the two ^{31}P environments of the complexes. However, the upfield signal at δ −6.8 in **2** appears fairly broad at 298 K, while those of **1** and $[\{Au(dppn)Cl\}_2](PF_6)_2$ remain sharp both at 298 and 203 K. The broadness of the ^{31}P signal in **2** at 298 K may suggest the presence of some fluxional behavior. Fluxionality in other related dinuclear d^9 complexes has also been reported.[18]

X-ray Crystal Structure Determination. Figures 1 and 2 show the perspective drawings of the complex cations of **1** and **2**, respectively. Selected bond distances and angles are summarized in Table 2. Both **1** and **2** consist of two distorted square planes about the two gold centers with a common Au−Au bond. The Au(1)−Au(2) bond distances in the respective bromo and iodo complexes **1** and **2** are 2.6035(8) and 2.6405(8) Å and are comparable to the Au^{II}−Au^{II} bond distance found in the chloro analogue [2.6112(7) Å].[7] Similar bond distances have also been observed in the dinuclear bis(ylide)gold(II) complexes.[2] The Au−Br distances in **1** [2.470(2)−2.534(2) Å] were found to be comparable to that in $[^nBu_4N]_2[Au_2(i\text{-mnt})_2Br_2]$ [2.510(8) Å],

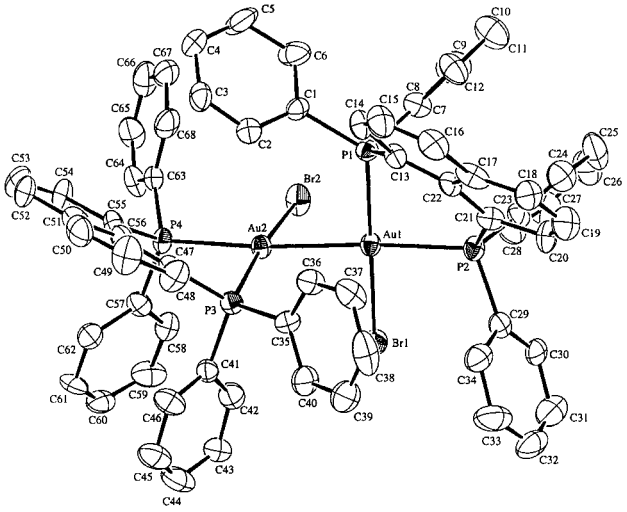

Figure 1. Perspective view of the complex cation of **1** with atomic numbering scheme. Hydrogen atoms have been omitted for clarity. Thermal ellipsoids were shown at the 35% probability level.

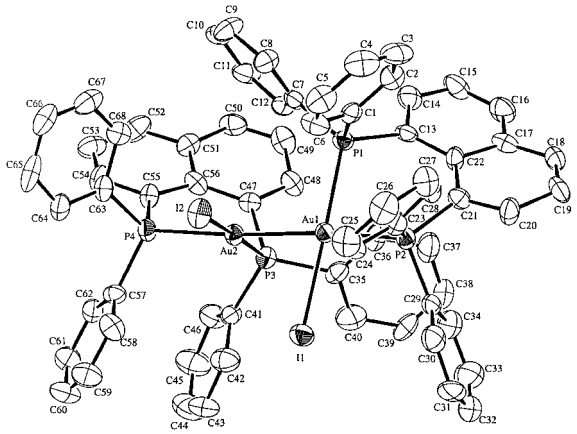

Figure 2. Perspective drawing of the complex cation of **2** with atomic numbering scheme. Hydrogen atoms have been omitted for clarity. Thermal ellipsoids were shown at the 35% probability level.

Table 2. Selected Bond Lengths (Å) and Angles (deg) with Estimated Standard Deviations (Esds) in Parentheses for $[\{Au^{II}(dppn)Br\}_2](PF_6)_2$ (**1**) and $[\{Au^{II}(dppn)I\}_2](PF_6)_2$ (**2**)

$[\{Au^{II}(dppn)Br\}_2](PF_6)_2$ (**1**)		$[\{Au^{II}(dppn)I\}_2](PF_6)_2$ (**2**)	
Au1−Au2	2.6035(8)	Au1−Au2	2.6405(8)
Au1−P1	2.389(4)	Au1−P1	2.341(4)
Au1−P2	2.400(4)	Au1−P2	2.399(3)
Au1−Br1	2.534(2)	Au1−I1	2.639(1)
Au2−P3	2.317(4)	Au2−P3	2.331(4)
Au2−P4	2.379(4)	Au2−P4	2.407(3)
Au2−Br2	2.470(2)	Au2−I2	2.638(1)
Au2−Au1−Br1	86.31(4)	Au2−Au1−I1	79.44(3)
Au2−Au1−P1	93.42(9)	Au2−Au1−P1	98.81(9)
Au2−Au1−P2	176.0(1)	Au2−Au1−P2	175.42(10)
Br1−Au1−P1	177.4(1)	I1−Au1−P1	178.24(9)
Br1−Au1−P2	89.7(1)	I1−Au1−P2	95.98(10)
P1−Au1−P2	90.5(1)	P1−Au1−P2	85.80(1)
Au1−Au2−Br2	79.09(4)	Au1−Au2−I2	78.75(3)
Au1−Au2−P3	98.73(9)	Au1−Au2−P3	100.36(9)
Au1−Au2−P4	174.7(1)	Au1−Au2−P4	173.50(1)
Br2−Au2−P3	171.8(1)	I2−Au2−P3	177.16(10)
Br2−Au2−P4	96.5(1)	I2−Au2−P4	95.30(10)
P3−Au2−P4	86.0(1)	P3−Au2−P4	85.7(1)

whereas the Au−I distances [2.638(1)−2.639(1) Å] in **2** are similar to that observed in $[Au(CH_2PPh_2CH_2)I]_2$ (2.693 Å).[2i,19] The Au−Au−P angles of 93.42(9)−98.81(9) and 176.00(1)−

(17) $^{31}P\{^1H\}$ NMR of $[\{Au(dppn)Cl\}_2](PF_6)_2$ (202 MHz, CD_2Cl_2): at 298 K, δ 32.5 (s), 13.5 (s); at 203 K, δ 31.6 (s), 12.0 (s).

(18) (a) Doonan, D. J.; Balch, A. L.; Goldberg, S. Z.; Eisenberg, R.; Miller, J. S. *J. Am. Chem. Soc.* **1975**, *97*, 1961. (b) Goldberg, S. Z.; Eisenberg, R. *Inorg. Chem.* **1976**, *15*, 535.

Table 3. Photophysical Data for $[\{Au^{II}(dppn)Cl\}_2](PF_6)_2$, **1**, and **2**

complex	medium (T/K)	λ_{abs}/nm (ϵ/dm^3 mol^{-1} cm^{-1})	λ_{em}/nm
$[\{Au^{II}(dppn)Cl\}_2]$ $(PF_6)_2$[a]	glass[b] (77)		555
	CH_2Cl_2 (298)	304 (22600), 354 (13700), 520 (44890)	574
1			
	glass[b] (77)		580
	CH_2Cl_2 (298)	310 (26090), 370 (15100), 544 (46530)	598
2	glass[b] (77)		685
	CH_2Cl_2 (298)	318 (19950), 348 (13920), 424 (12290), 476 (8840), 602 (17500)	*c*

[a] From ref 7. [b] CH_2Cl_2−EtOH−MeOH (1:8:2 v/v). [c] Nonemissive.

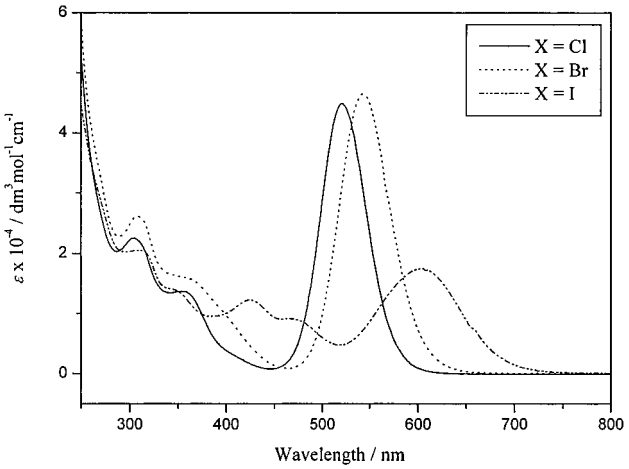

Figure 3. Electronic absorption spectra of $[\{Au^{II}(dppn)X\}_2](PF_6)_2$ in dichloromethane at 298 K.

175.42(10)° and the X−Au−P angles of 89.70(1)−95.98(10) and 177.40(1)−178.24(9)° in both **1** and **2** show only slight deviations from 90 and 180° expected for an ideal square planar geometry at the gold center.

Photophysical Studies. The UV−visible absorption spectra of the bromo complex **1** and its chloro analogue, $[\{Au(dppn)Cl\}_2]^{2+}$, are dominated by intense absorption bands at ca. 300−370 and 520−550 nm, with extinction coefficients in the order of 10^4 dm^3 mol^{-1} cm^{-1}. This indicates that the electronic transitions associated with these absorption bands are both spin and orbital allowed. Similar to the chloro analogue, the absorption bands at ca.300−370 nm are assigned as the $\pi \rightarrow \pi^*$ and $\sigma \rightarrow \pi^*$ transitions within the naphthyl ring.[7] The UV−visible absorption spectra of the bromo and iodo complexes **1** and **2** and their chloro analogue in dichloromethane at room temperature are shown in Figure 3. Their photophysical data are collected in Table 3. The UV−visible absorption spectrum of the iodo complex **2** also shows high-energy ligand-centered absorptions at ca. 310−350 nm. In the visible region, apart from the intense band at 602 nm, additional bands at ca. 420 and 470 nm are observed. The possibility that these bands are a result of impurities such as I_3^- has been eliminated since I_3^- does not absorb at such a low energy. It is also interesting to note that the low-energy absorption band at 602 nm not only shifts to the red relative to the chloro and bromo analogues but also is less intense than the chloro and bromo counterparts by a factor of over 2. It is likely that some splitting of the bands has occurred in **2**. With reference to previous spectroscopic works on dinuclear Au(II) systems by us[7] and others,[2−4] the low-energy absorption band in the region of 520−602 nm, which gives rise to the distinctive purplish blue color of these dinuclear Au(II) complexes and shows an energy order $[\{Au(dppn)Cl\}_2]^{2+}$ [520 nm (2.4 eV)] > **1** [544 nm (2.3 eV)] > **2** [602 nm (2.1 eV)], may tentatively be assigned as a metal-centered $d_\sigma \rightarrow d_{\sigma^*}$ transition. However, the $[\{Au(dppn)X\}_2]^{2+}$ system, unlike the $[Au_2(i\text{-mnt})_2X_2]^{2-}$ series[4a] in which the energy of the absorption bands for the chloro, bromo, and iodo analogues [X = Cl, 550 nm (2.3 eV); X = Br, 586 nm (2.1 eV); X = I, 640 nm (1.9 eV)] follows the trend in the Au−Au distances [X = Cl, 2.550-(1) Å; X = Br, 2.570(5) Å], does not show a simple relationship between its low-energy absorption energies and the Au−Au distances. The Au−Au distances in the order **1** [2.6035(8) Å] < $[\{Au(dppn)Cl\}_2]^{2+}$ [2.6112(7) Å] < **2** [2.6405(8) Å] should predict a $d_\sigma \rightarrow d_{\sigma^*}$ transition energy in the order **1** > $[\{Au(dppn)Cl\}_2]^{2+}$ > **2**. However, such a trend is not observed. Instead, a trend more in line with the ionization energies of the halogen atom is observed. It is likely that the low-energy absorption in these dinuclear Au(II) complexes is not a pure metal-centered $d_\sigma \rightarrow d_{\sigma^*}$ transition but has some mixing of a halide-to-gold ligand-to-metal charge transfer (LMCT) character. This is especially the case when the energy of the donor orbital of the ligand such as I^- is comparable to that of $5d_z^2$(Au), such that a more complex $d_\sigma(Au_2)/p_\pi(X) \rightarrow d_{\sigma^*}(Au_2)$ spectrum is expected. Similar observations have been reported in the $[Pt_2(pop)_4X_2]^{4-}$ and binuclear rhodium(II) isocyanide complexes.[20,21] At first sight, the involvement of a LMCT character in the present case may be less than that of the $[Pt_2(pop)_4X_2]^{4-}$ system, since a larger energy dependence on the nature of the halogen was observed in the latter [X = Cl, 282 nm (4.4 eV); X = Br, 305 nm (4.1 eV); X = I, 338 nm (3.7 eV)].[20] However, another possibility for the relatiely small red shift observed in absorption energy from the chloro to the bromo analogue may result from a mixing of the $p_\sigma(P) \rightarrow d_{\sigma^*}(Au_2)$ LMCT character into the transition, similar to that observed in the $[Mo_2(PMe_3)_4X_4]$ system.[22] In view of the short Au−Au distances, the $d_\sigma(Au_2) \rightarrow d_{\sigma^*}(Au_2)$ transition should occur at higher energies. Thus we favor the assignment of the low-energy absorption to involve substantial LMCT character, probably with mixing of the $p_\pi(X) \rightarrow d_{\sigma^*}(Au_2)$ and $p_\sigma(P) \rightarrow d_{\sigma^*}(Au_2)$ characters.

Excitation of dichloromethane solutions of **1** and **2** at λ > 400 nm at 77 K glasses resulted in emission, with lifetimes of less than 10 ns. The overlaid emission spectra of the complexes in 77 K glasses are depicted in Figure 4. The emission spectra

(19) Clark, R. J. H.; Tocher, J. H.; Fackler, J. P., Jr.; Neiar, R.; Murray, H. H.; Knachel, H. *J. Organomet. Chem.* **1986**, *303*, 437.

(20) (a) Che, C. M.; Butler, L. G.; Grunthaner, P. J.; Gray, H. B. *Inorg. Chem.* **1985**, *24*, 4662. (b) Roundhill, D. M.; Gray, H. B.; Che, C. M. *Acc. Chem. Res.* **1989**, *22*, 55. (c) Shin, Y. K.; Miskowski, V. M.; Nocera, D. G. *Inorg. Chem.* **1990**, *29*, 2308.

(21) (a) Miskowski, V. M.; Smith, T. P.; Loehr, T. M.; Gray, H. B. *J. Am. Chem. Soc.* **1985**, *107*, 7925. (b) Rice, S. F.; Gray, H. B. *J. Am. Chem. Soc.* **1981**, *103*, 1593. (c) Stiegman, A. E.; Rice, S. F.; Gray, H. B.; Miskowski, V. M. *Inorg. Chem.* **1987**, *26*, 1112.

(22) Miskowski, V. M.; Gray, H. B.; Hopkins, M. D. *Inorg. Chem.* **1992**, *31*, 2085.

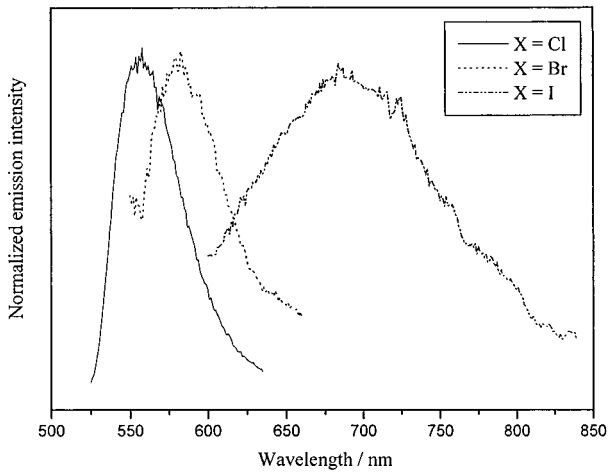

Figure 4. Normalized emission spectra of $[\{Au^{II}(dppn)X\}_2](PF_6)_2$ in glass medium at 77 K.

show structureless band at 555−685 nm. Complex **1** and $[\{Au(dppn)Cl\}_2](PF_6)_2$ also emit in dichloromethane solution at 298 K. Similar to that observed in the UV−visible absorption spectra, a red shift in the emission energy [X = Cl, 555 nm (2.23 eV); X = Br, 580 nm (2.14 eV); X = I, 685 nm (1.81 eV)] in 77 K glasses has been observed. An assignment of these low-energy emissions to states of a $d_\sigma(Au_2)/p_\pi(X) \rightarrow d_{\sigma^*}(Au_2)$ origin, with substantial LMCT character, probably with mixing of $d_{\pi^*} \rightarrow d_{\sigma^*}$ and $p_\sigma(P) \rightarrow d_{\sigma^*}(Au_2)$ characters, is suggested.

Conclusion. A series of novel dinuclear gold(II) complexes with unsupported Au(II)−Au(II) bond have been synthesized and structurally characterized. The complexes have been shown to exhibit interesting photophysical properties. Upon the change of the coordinating halogen atoms, the origin of the low-energy emission has been probed and suggested as derived from states of a $[d_\sigma(Au_2)/p_\pi(X) \rightarrow d_{\sigma^*}(Au_2)]$ metal-centered/LMCT transition, mixed with $p_\sigma(P) \rightarrow d_{\sigma^*}(Au_2)$ LMCT character.

Acknowledgment. V.W.-W.Y. acknowledges financial support from the Research Grants Council and The University of Hong Kong, C.-K.L., the receipt of a Postgraduate Studentship, administered by The University of Hong Kong, and C.-L.C., the receipt of a Croucher Studentship and Scholarship, administered by the Croucher Foundation, and the Sir Edward Youde Postgraduate Fellowship administered by the Sir Edward Youde Memorial Fund Council. Helpful discussions with Dr. V. M. Miskowski are gratefully acknowledged.

Supporting Information Available: Tables (in CIF format) giving atomic coordinates, anisotropic thermal parameters, bond lengths, and bond angles for complexes **1** and **2**. This material is available free of charge via the Internet at http://pubs.acs.org.

IC010744T